

3-D ANALYSIS OF HIGH DENSITY BRUSH STIFFNESS WITH FRICTION-PRESSURE COUPLING

Mahmut F. Aksit
Sabanci University, Istanbul, Turkey, 34956

ABSTRACT

Achieving efficient sealing around high speed rotating bodies poses real engineering challenges. In recent years, dense brush structures found common use in turbomachinery sealing applications. As they maintain their flexibility at elevated temperatures, which are typical in gas turbines, high density brush seals made of super-alloy bristles found popularity among engine designers. Inherent flexibility of brush seals allows fibers to compact under pressure load. Due to the frictional interaction between the fibers and the backing plate as well as within the fibers themselves, brush seals are known to exhibit pressure stiffening and hysteresis behavior. While hysteresis affects seal performance after a rotor excursion, pressure stiffening is critical in determining heat generation and seal wear during hard rubs. Typically brush-rotor contact occurs at very high surface speeds. If not managed properly, high contact loads may result in extreme wear and damage to rotor. In order to ensure engine operational safety brush seal stiffness should be controlled through seal design and detail analysis. In addition to the physical complexity of these dense brush structures, frictional contacts among the bristles themselves, between the bristles and the support plates, and between the bristles tips and the high speed rotor further increase the analysis complexity, and make it a major undertaking if not impossible. The complicated nature of bristle behavior under various combinations of pressure load and rotor interference requires computer analysis to study details that may not be available through analytical formulations. This work presents a 3-D computational brush seal structural FE model that can be used to calculate bristle forces. The analysis includes a representative brush segment with bristles formed by 3-D beam elements. Bristle interlocking and frictional interactions (interbristle, bristle-backing plate and bristle-rotor) are included to better simulate pressure-stiffness coupling. The results indicate that rotor interference has some effect on seal tip forces in the absence of any pressure loading. However, upon application of small pressure loads, seal stiffness is generally dominated by pressure-stiffness coupling.

INTRODUCTION

The brush seal consists of a set of fine diameter fibers densely packed between retaining and backing plates. As illustrated in Fig. 1, the backing plate is positioned downstream of the bristles to provide mechanical support under differential pressure loads. The bristles touch the rotor with a lay angle in

the direction of the rotor rotation allowing them to bend rather than buckle during rotor excursions. Last few decades, brush seals have been extensively used in secondary flow sealing in turbo-machinery applications. They have demonstrated excellent leakage characteristics.

Differential pressure across a seal pushes the bristles against the backing plate. Due to mechanical interlocking as well as the frictional mechanisms, bristles stick to one another. The bristle pack also sticks to the backing plate. The frictional resistance at the backing plate causes a large increase in the contact loads at the rotor surface. When subjected to a radial interference under a sealing pressure, the seal feels much stiffer than it does without any pressure load. This leads to increased wear rates which reduce the seal life.

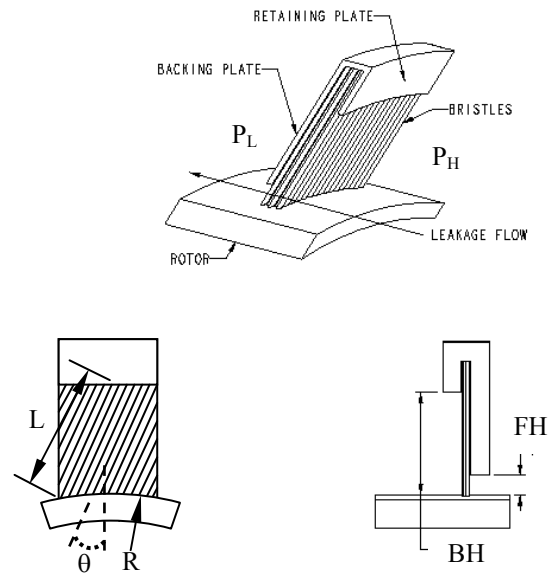


Fig. 1 Brush seal geometry.

FINITE ELEMENT MODEL

During operation, bristles experience deflection in a radial plane due to rotor excursion, while they bend axially under pressure load. Therefore, a three-dimensional solution is required for a proper brush seal analysis. The model consists of

a representative bristle bundle with a backing plate and a rotor surface (Fig. 2). Every bristle is defined by a number of 3-D quadratic beam elements. The rotor and the backing plate are defined as rigid surfaces. A representative backing plate is placed behind the first bristle row of bristles. In addition to the main design parameters defined in Fig. 1, analysis requires information on material properties, bristle diameter and friction coefficients for various contact locations.

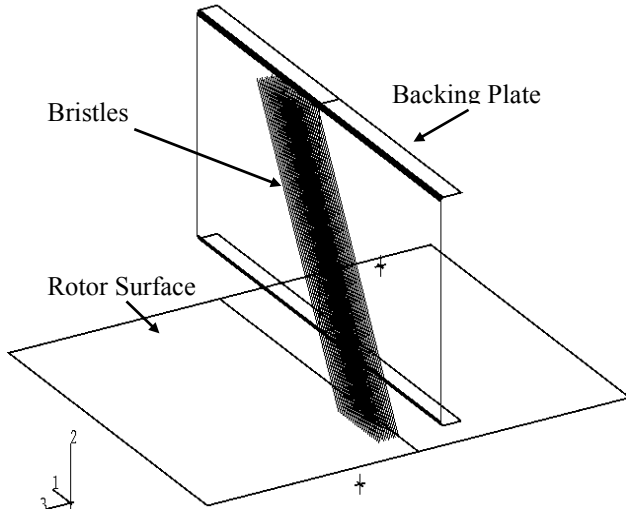


Fig. 2 The 3-D finite element model of a brush segment.

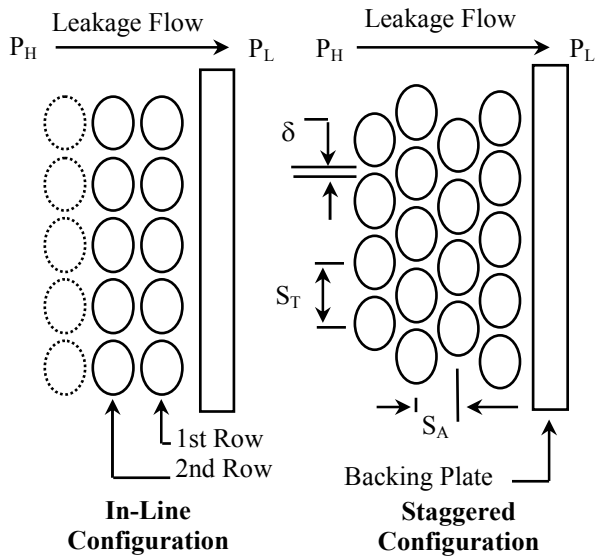


Fig. 3 Possible bristle layouts in circumferential plane.

Modeling of bristle spacing involves layout and proximity. Within the brush pack two types of bristle layouts can be considered in the circumferential plane, namely, in-line or staggered (Figs. 3 and 4). The actual spacing will be a mixture of these two. Microscopic inspections reveal that in a typical seal most of the bristles tend to stay in a staggered configuration. Therefore, the presented analysis incorporates the staggered configuration to achieve a better simulation of the real case. As manufacturing aims for the highest attainable density, bristle spacing usually gets close to the minimum

geometrically possible. Crudgington et al [1] reported 15% blooming in thickness at free state. However, current model considers 25% blooming for the axial spacing, S_A . Extra axial space helps reduce solver problems in the initial phase of the analysis. These values define initial spacing for the presented model where bristles immediately compact upon application of pressure load. Since there is no coupled CFD analysis, applied aerodynamic loading does not change with spacing. On the other hand, spacing is extremely important for brush seal leakage and flow models.

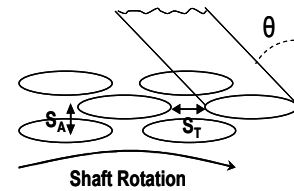


Fig. 4 Footprints of bristles on the shaft surface.

As for the tangential spacing (S_T), the analysis defines 5% of the minimum geometric center-center distance as the gap (δ) to represent common seal density of ~ 2000 bristles per inch of rotor circumference.

Depending on the bristle diameter a standard density brush seal can have 8-12 bristle rows in rotor axial direction. The model has been successfully tested up to 20 bristles in a row, and up to 16 bristles rows without any convergence or numerical stability problems. This allows simulation capability from standard to double density seal designs.

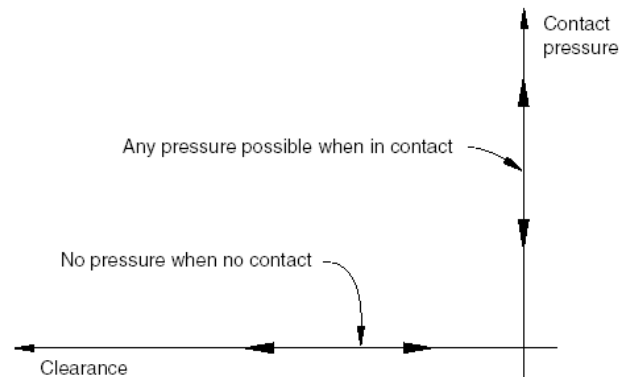


Fig. 5 Pressure-clearance relationship for bristle-rotor contact surface pairs.

Contact Definitions

Based on the physical nature of the interactions, three types of contacts are modeled. The interaction between the bristle tips and the rotor is defined as a rigid surface contact where rotor is infinitely rigid while bristles are allowed to deform. In this interaction, contact loads are transmitted as soon as the tip node of a bristle touches the rotor surface. Since the rotor is defined as the rigid surface, it represents the master surface in the bristle-rotor contact pairs. The first two or three beam elements at the tip of each bristle are defined as stress-displacement rigid

surface elements which are coupled with the rotor surface. These elements represent the slave surface. They are allowed to be compliant and deformable. The nodes of the slave surface can not penetrate into the master surface. Therefore, contact direction is always normal to the master surface. For bristle-rotor contacts, pressure-clearance relationship is defined as illustrated in Fig. 5. This allows contact pressure to build-up only after the tip node of a bristle touches the rotor.

The interaction between the first row of bristles and the backing plate is similar to that of the rotor contact. However, contact is detected when bristle center nodes are at a distance of bristle radius away from the backing plate (see Fig. 6). This type of pressure-clearance relationship is called softened contact. Inter-bristle interactions involve deformation of both of the bodies. Therefore, they are modeled using slide lines. In a slide line contact, elements of one of the interacting bodies slide against the line defined by the nodes of the other body. This line of interaction is defined by attaching slide line contact elements to the surface of one of the bodies, and associating these elements with a set of nodes on the other surface. Fig. 7 illustrates the slide line concept. Relative motion along the line of interaction can be arbitrarily large. But relative motions out of the plane containing the line of interaction are assumed to be comparably small.

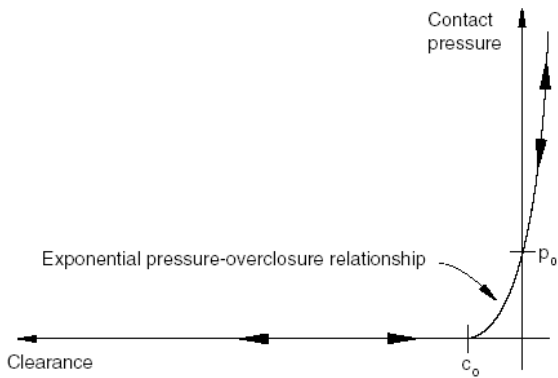


Fig. 6 “Soft Contact” pressure-clearance relationship for bristle-backing plate and bristle-bristle contact surface pairs.

If the interacting bodies are cylinders/tubes, as the case here, through the use of special slide line contact elements, the relative motion is allowed to be along a curve of contact. In this case, the contact direction is normal to the slide line in the direction of the smallest distance between the surfaces of the cylinders (bristles). For a bristle couple, all the nodes in one of the bristles form the slide line. The corresponding second order slide line contact elements on the other bristle are defined. Fig. 8. illustrates the use of slide lines between the bristles. The model does not include the first node at the free tip in the contact elements to avoid over constraining the tip node as it is also in contact with the rotor surface. The last two nodes at the top of the bristles are also spared, as they would be over constrained. Bristles are fixed at this end, and these nodes will not see any sizable sliding. The contact is detected at a bristle diameter distance between the two node-sets located at the bristle centerlines. Both inter-bristle and backing plate contacts

incorporate additional surface roughness involved when calculating contact detection distances.

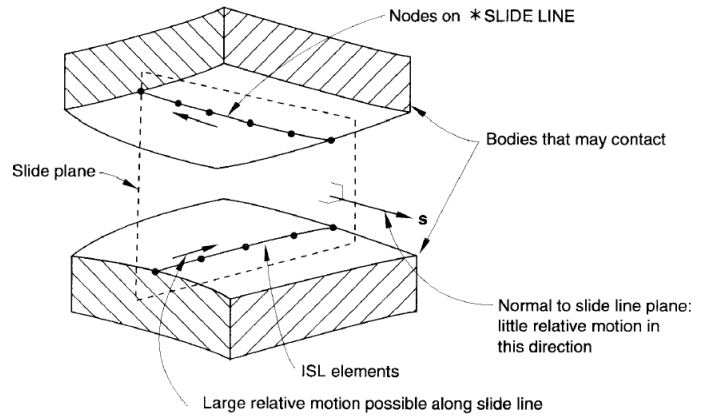


Fig. 7 Slide line concept in a contact pair.

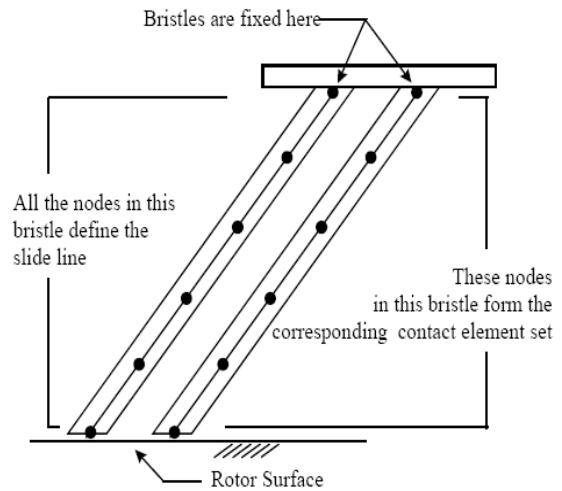


Fig. 8 Application of slide lines in a bristle pair.

Friction Modeling

The analysis incorporates classical isotropic coulomb friction model for all contacts. When two bodies are in-contact both shear and normal forces are transmitted across the interface. The incorporated coulomb friction model assumes that no relative motion occurs until the equivalent frictional shear stress reaches a threshold value which depends on the friction coefficient defined for that contact. The critical stress, τ_{crit} , is proportional to the contact pressure, p , in the form

$$\tau_{crit} = \mu p$$

where μ is the friction coefficient (Fig. 9). This standard isotropic constant friction model facilitates an easier solution to the complicated frictional contact problems. The reported values of friction coefficient for common Haynes 25 fiber widely vary from 0.08 to 0.47 under different test conditions. Crudginton et al [1] obtained steady readings of 0.28 when running against stainless steel. This value is taken as an average overall friction coefficient in the presented analysis.

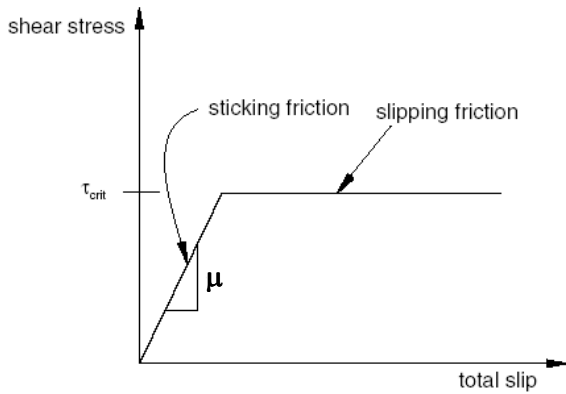


Fig. 9 Friction model used in the analysis.

Boundary Conditions

Proper application of the boundary conditions is necessary for an accurate analysis. Due to the strong pressure-friction coupling present in brush seals, loading sequence is critical. If pressure is applied after a prescribed radial interference, the contact loads will be lower than the case where a pressure is applied before the rotor interference. Most real applications involve the latter case. The analysis updates pressure load distribution at every displacement increment as radial locations of elements change during rotor interference.

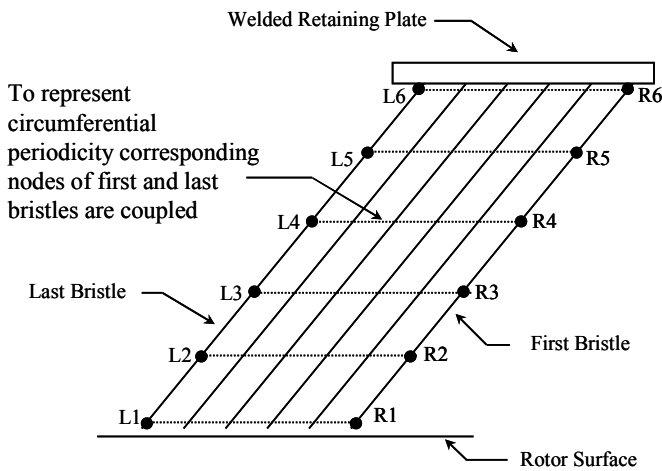


Fig. 10 Coupling of end bristle nodes in a row in the analysis.

To represent bristle clamping and the weld at the periphery, all 6 degrees of freedom (both translations and rotations) for top node of each bristle is constrained. Frictional contact defined at backing plate limits axial bristle motion. Bristles are free to slide on the backing plate or to bend below the fence height under axial pressure load. Frictional contact defined at bristle tips allows bristles to slide tangentially, or to bend axially when rotor surface is moved towards the brush pack under pressure. To provide circumferential periodicity, first and last bristles in each row are coupled in a master-slave relationship (Fig. 10). The last bristle at every row experiences

a pull from the first, instead of the resistance from the rest of the bristles behind it. Similarly, this load transfer allows the first bristle to experience a pull from the last bristle rather than a push by the rest of the bristles before it. Seal-rotor interference is simulated by applying radial displacements to the rigid body node representing the rotor surface. Rotor surface can also be assigned circumferential velocity to simulate actual rotor rotation in service.

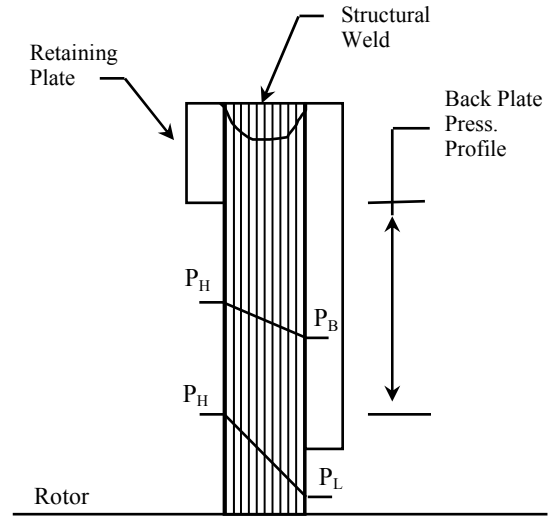


Fig. 11 Pressure boundary conditions.

Pressure distribution in and around the bristle pack defines the axial and radial pressure loads on each bristle. For accurate pressure boundary condition both axial and radial pressure profiles are needed. Measurements by Bayley et al [2] and observations by Braun et al. [3] suggest almost a linear axial pressure drop. Therefore, the model incorporates a linear axial pressure drop within the bristle pack as illustrated in Fig. 11. An arbitrary bristle in the middle of the pack is loaded by a prescribed axial force due to leakage flow (axial pressure drop) while it is also subjected to the contact forces transmitted by the adjacent bristles. Axial pressure difference across the bristle pack varies with the radial position along the backing plate while portion of the seal at the fence height region experience the maximum pressure load. Radial pressure profile can be estimated by pressure variation along the backing plate. Pressure at the backing plate (P_B) is close to upstream pressure (P_H). It quickly drops to downstream pressure (P_L) near the inner edge of the backing plate. The model uses a radial pressure profile based on the data provided by Bayley et al. [2] and Turner et al. [4].

RESULTS AND DISCUSSION

Before studying pressure-stiffness coupling, the analysis has been compared with experimental data and other analysis results available in the literature for validation purposes. Experimental stiffness measurements provided by Crudginton [1] have been taken by bringing a shoe, shaped to the curvature of the bristle bore, into contact with the bristles and then displacing it further to simulate radial rotor interference. The tests have been performed without any pressure load on seals.

To compare with the experimental results both analyses (analysis by Crudginton [1] and the current analysis) have been conducted without pressure load application. As illustrated in Fig. 12, both analyses predict hysteresis behavior between loading and unloading periods as observed during testing. The beam analysis has been provided to serve as a bench mark. The beam calculation assumes each bristle as a simple cantilever estimating the tip force for induced deflection.

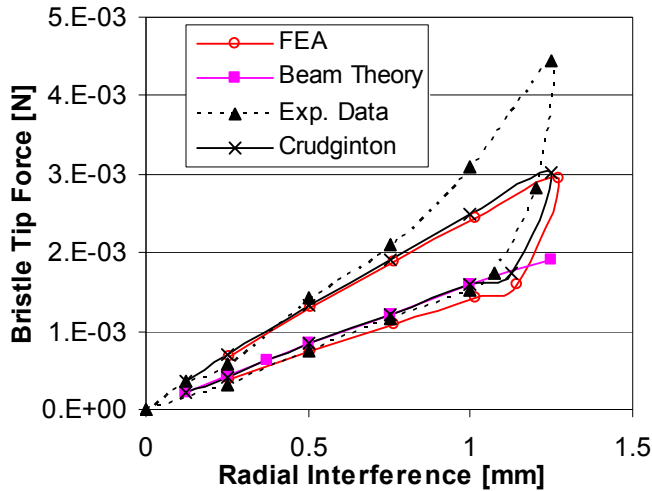


Fig. 12 Comparison of analysis results with Crudginton’s results [1] and experimental data.

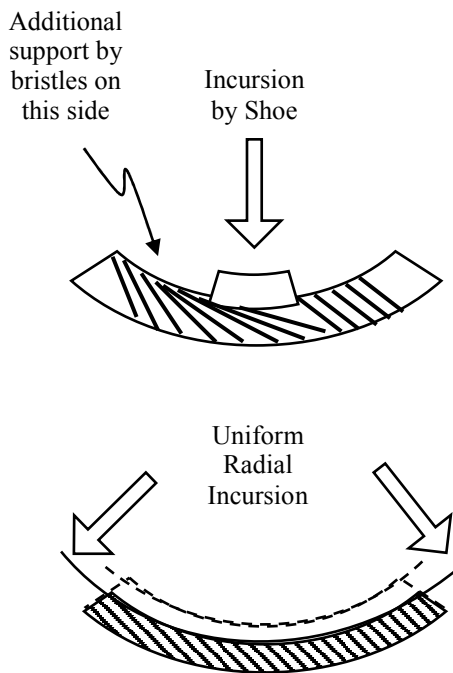


Fig. 13 Nonuniform bristle deflection during shoe pressing tests explains nonlinear increase in force measurements.

Both analyses predict almost identical bristle tip force reactions. On the experimental side, verification analysis results

perfectly match at low interference levels up to 0.5 mm. At large interference values, however, the analysis underestimates the measured bristle tip force values. The measured nonlinear increase at large deflections is somewhat expected. As illustrated in Fig. 13, measuring seal stiffness by pressing only at a segment involves additional resistance and support from one side of the bristle segment after some packing has been accomplished. In the experiment, displacement is applied only to a segment of the bristle. However, the analysis simulates uniform radial interference due to the circumferential periodicity boundary condition applied. As shown in Fig. 13, uniform radial interference eliminates unrealistic end effects involved in segment testing.

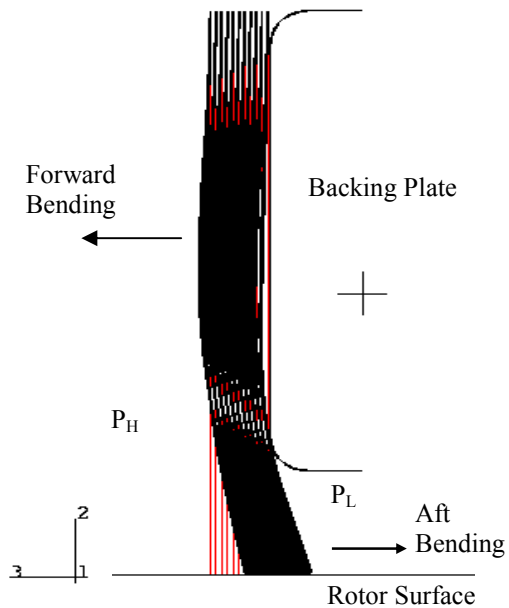


Fig. 14 Modeled seal behavior under differential pressure load.

After verification runs and analyses without pressure loads, a series of analyses has been conducted to study pressure-stiffness coupling in brush seals. When pressure load is applied, the analysis accurately models compaction of bristles with all the frictional contact definitions incorporated. The cross-sectional detail shown in Fig. 14 confirms axial bending of bristles below the backing plate, as expected.

Pressure-stiffness effects are studied at various pressure levels. Since loading sequence changes bristle contact loads, all of the analyses have been conducted using pressure-interference sequence. This represents real applications better as in most real life applications pressure load is present when interference starts occurring. When pressure is applied first, bristles are already compacted, and seal is stiffened. Therefore, application of radial interference will result in higher contact loads. The analyses have been performed at four different pressure loads. A series analyses has been performed for each pressure level. After the pressure load has been applied, radial interference has been increased in five increments up to 1.2 mm. Then, without removing pressure load, the interference is gradually removed. Bristle tip forces are calculated (and presented in Fig. 15) for each pressure and interference combination. The results reveal interesting seal behavior.

Overall, findings indicate that seal-rotor contact force is determined by pressure load level. Even application of a small 34.5 kPa (5 psi) pressure load compacts the bristles, and pushes them against the backing plate. This eliminates the free bristle height as a determining factor for bristle tip force, as bristles are not free any more.

remains very limited for the analyzed seal design with standard backing plate geometry.

REFERENCES

- [1] Crudgington, P. F., and Bowsher, A., "Brush Seal Pack Hysteresis," (2002) AIAA Paper No. AIAA-2002-3794.
- [2] Bayley, F. J., and Long, C. A., "A Combined Experimental and Theoretical Study of Flow and Pressure Distributions in a Brush Seal," ASME J. Eng. Gas Turbines Power, 115, No. 2, (1993) 404-410.
- [3] Braun, M. J., Hendricks, R. C., and Canacci, V., "Flow Visualization in a Simulated Brush Seals," (1990) ASME Paper No. 90-GT-217.
- [4] Turner, M. T., Chew, J. W., and Long, C. A., "Experimental Investigation and Mathematical Modeling of Clearance Brush Seals," ASME J. Eng. Gas Turbines Power, 120, No. 3, (1998) 573-579.

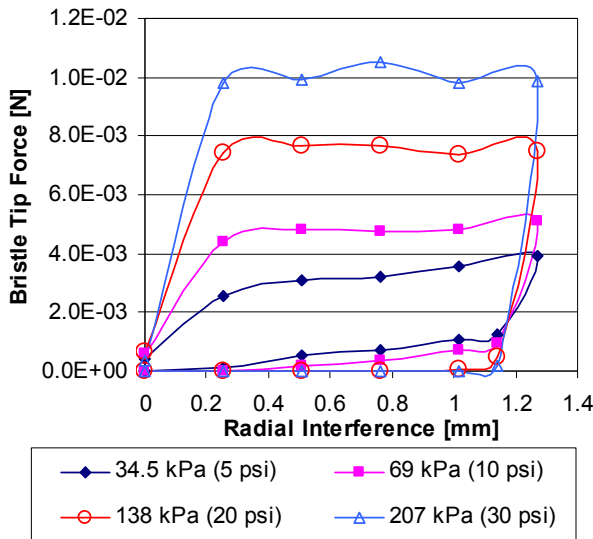


Fig. 15 Bristle-Rotor contact force under different pressure-interference load combinations.

7. CONCLUSION

As brush seal applications get more and more challenging detailed understanding of brush seal contact loads and pressure-stiffness coupling behavior is needed. The presented computational model provides a reliable means to study brush seal contact forces under various pressure-interference load combinations. The analysis results indicate the following conclusions:

- Application of even a small 34.5 kPa (5 psi) pressure load compacts the bristles, and pushes them against the backing plate.
- Pressure load level dictates the magnitude of the bristle tip force. When seal is under pressure load, rotor contact forces do not change with radial interference. However, contact forces increase with increasing pressure load.
- Classical stiffness definition (rotor contact force / radial interference) can not be used as a measure of seal stiffness for pressure loaded cases. Since contact load remains almost constant with radial interference, using such formulations will cause seal stiffness to decrease with increasing interference. Therefore, comparing seal contact forces at a bench mark pressure level will provide a better comparison between various seal designs.
- Presented analysis can accurately simulate hysteresis and bristle hang-up behavior. When radial interference is removed under pressure, bristle tip forces quickly drop to zero indicating a seal hang up. The amount of blowdown